Research Paper

Fluorinated Benzyloxalamides: Glide Docking, Pharmacophore Mapping, Synthesis and *In Vitro* Evaluation as Potential Cholesteryl Ester Transfer Protein Inhibitors

R. ABU KHALAF*, D. SABBAH, E. AL-SHALABI, B. IKHMAIS, W. NASER AND G. ALBADAWI

Department of Pharmacy, Faculty of Pharmacy, Al-Zaytoonah University of Jordan, Amman 11733, Jordan

Worldwide, cardiovascular disease is considered a major cause of death and disability. Age, sex, blood pressure, total cholesterol, high-density lipoprotein cholesterol, smoking and diabetes contribute in the development of the disease. Hence, high-density lipoprotein cholesterol modulation using cholesteryl ester transfer protein inhibitors could have a great role in reducing cardiovascular disease risk and mortality. In this work, ten new benzyloxalamides 8a-j were synthesized and characterized targeting the cholesteryl ester transfer protein inhibition. Biological study results showed that compound 8f had the greatest activity with a percentage inhibition of 64.1 at a concentration of 10 µM and an half-maximal inhibitory concentration of 2.1 µM. Functional moieties of 8a-j matched the cholesteryl ester transfer protein inhibitors pharmacophoric features; mainly the aromatic and hydrophobic ones. Moreover, Glide docking revealed that the targeted compounds lodge the binding site of cholesteryl ester transfer protein and are surrounded by hydrophobic liner. Benzyloxalamides can serve as lead scaffold for the development of cholesteryl ester transfer protein inhibitors.

Key words: Benzyloxalamides, cardiovascular disease, cholesteryl ester transfer protein, glide docking, inhibitors, pharmacophore model

Cardiovascular Disease (CVD) is the leading cause of mortality worldwide[1]. Observational epidemiologic studies have reported that low plasma concentration of High-Density Lipoprotein Cholesterol (HDL-C) is an independent risk factor for occlusive CVD, including Coronary Heart Disease (CHD) and ischemic stroke[2]. Poor eating habits, smoking and inactivity are environmental factors that increase the prevalence of CVD risk phenotypes, especially hypercholesterolemia[3,4]. On the other hand, dyslipidemia is a disease with abnormal amount of blood lipids[5]. It could be primary or secondary to other causes like diabetes, obesity, cigarette smoking, sedentary lifestyle or consuming high fat foods[6]. Dyslipidemia can be primarily controlled by healthy diet and exercise. Still, medications can be necessary if these modifications fail[7]. Furthermore, lipid profile has considerable scope for improvement in patients with dyslipidemia[8].

Current findings show that higher levels of LDL-C and lower levels of HDL-C are associated with increased CVD risk. Clinicians have been able to lower morbidity and mortality related to major cardiovascular events through lowering of LDL-C with 3-Hydroxy-3-Methylglutaryl Coenzyme A (HMG-CoA) reeducates inhibitors (statins)[9]. Despite statin use, CVD risk persists. Thus, it is essential to investigate other means of lowering CVD risk. Studies have clearly shown that a low HDL-C level is a strong and independent risk factor for the development of CVD[10]. This suggests that further HDL-C modulation could have a large role in reducing CVD risk and mortality. Search for HDL-C modulator makes Cholesteryl Ester Transfer Protein (CETP) inhibition a thrilling possibility of pharmacotherapy[9].

HDL-C is largely generated in the liver and is an essential player in Reverse Cholesterol Transport (RCT)[11,12]. RCT is the process in which HDL macromolecules absorb free cholesterol from

***Address for correspondence**
E-mail: reema.abukhalaf@zuj.edu.jo

This is an open access article distributed under the terms of the Creative Commons Attribution-NonCommercial-ShareAlike 3.0 License, which allows others to remix, tweak, and build upon the work non-commercially, as long as the author is credited and the new creations are licensed under the identical terms

Accepted 02 December, 2022
Revised 27 December 2021
Received 08 April 2020
Indian J Pharm Sci 2022;84(6):1476-1487

the periphery and transport it back to the liver for metabolism. It is suggested that this is the mechanism by which HDL-C is cardio-protective and anti-atherogenic[11,13]. However, additional studies have demonstrated anti-oxidative[14], anti-inflammatory[14], endothelial protective[15] and anti-gluconeogenic[16,17] properties of HDL-C which may also be contributing to its benefit[16-18].

CETP transfers the cholesteryl esters from HDL to apolipoprotein B-containing particles in exchange for triglycerides[19] and has been considered to be a new drug target for increasing HDL-C levels. Human CETP may play an important role in the development of atherosclerosis mainly by decreasing HDL-C levels and increasing the accumulation of macrophage-derived foam cells[20]. In individuals with essentially normal lipid levels, CETP con-centration is about 1-4 µg/ml, while the concentration may be 70 %-80 % higher among those with hyperlipidemia[21].

Large human genetic studies have shown that single nucleotide polymorphisms in the CETP gene that are associated with increased HDL and reduced LDL-C are associated with reduced CHD[22]. While, genetic variants in the CETP gene that were associated with altered HDL metabolism but not lower LDL cholesterol levels had no association with CVD risk[23].

CETP is a hydrophobic glycoprotein of 476 amino acids. Its crystal struc¬ture reveals a banana-shaped molecule with N-and C-terminal β-barrel domains, a central β-sheet and a 60 Å long hydrophobic central cavity, which can accommodate two cholesteryl ester molecules and communicates with two pores near the central β-sheet domain. The pores are occupied by two phospholipid molecules and could interact with the lipoproteins[24]. CETP transports cholesterol and triglycerides between apoA- and apoB-containing lipoproteins. The direction of transport may be under the influence of current plasma lipid concentrations[25]. CETP may be adaptive by elevating plasma levels in response to an elevated peripheral cholesterol efflux[26]. CETP-mediated cholesterol transfer from LDL-C and Very-LDL-C (VLDL-C) to HDL-C is thought to be anti-atherogenic[27,28].

Currently, four drugs make up the CETP inhibitor drug class under investigation; torcetrapib (Pfizer), dalcetrapib (Roche), evacetrapib (Eli Lilly and Co.) and anacetrapib (Merck and Co.). When the first three CETP inhibitors were added to background statin therapy, their use either increased the risk of CVD and death (as torcetrapib[29]) or had neutral outcomes (as dalcetrapib[30] and evacetrapib[31]). These failures quenched even the hope of benefit for the remaining CETP inhibitor, anacetrapib[32]. Studies in mildly hypercholesterolemia subjects treated with anacetrapib have shown that the reduction in VLDL and LDL results from an increase in the catabolism[33-35]. Two additional drugs are in early stages of development, BAY60-552164[36] and JNJ-28545595[37]. Core structure of torcetrapib, anacetrapib and evacetrapib are all tetrahydroquinoline inhibitors comprised of 3,5-bis-trifluoromethylbenzyl groups. These compounds have been modified by a biaryl moiety (as in anacetrapib) or with methyl tetrazole and cyclohexane carboxylic acid side chains (as in evacetrapib). While dalcetrapib is made up of an ortho-thioanilide core[38].

Recently, it has been proposed that CVD benefit from CETP inhibition through the reduction in LDL-C, rather than the elevation in HDL-C. In addition, CETP inhibitors have been shown to improve glucose tolerance, lower the new-onset diabetes risk and insulin sensitivity. The newest-generation CETP inhibitor obicetrapib has achieved significant reduction of LDL-C up to 45 %. Obicetrapib could become the first CETP inhibitor as add-on therapy for patients not reaching their guideline LDL-C targets[39].

Several natural products have therapeutic potential in lipid disorders. As an example, the *Garcinia mangostana* L. pericarp and seed contain flavonoids, anthocyanins and benzophenones derivatives. It has remedial benefits for obesity and lipid metabolism disorder along with their complications[40]. Moreover, from the fungus *Engleromyces goetzii* culture, novel cleistanthane-derived diterpene was isolated and found to have inhibitory activity against CETP[41]. Additionally, crocin supplements, that is given to patients suffering from metabolic syndrome, considerably reduced the CETP and increased HDL-C after treatment[42]. Further research finds that saffron, a natural product with a wide variety of medical uses, could be a potent lead compound for new drug discovery in the treatment of CVD[43].

Several series of CETP inhibitors were developed in our research lab including benzylideneamino-

methanones[44], benzylamino-methanones[45], benzene sulfonamides and toluene-4-sulfonic acid esters[46], fluorinated benzamides[47], chlorobenzyl benzamides[48] and substituted benzamides[49-51]. So as to understand better the structure activity relationship of the formerly discovered hits[49], different analogues were prepared by varying the aromatic substitution (p-CF_3, p-OCF_2CF_2H) then biological activity of these compounds was evaluated.

MATERIALS AND METHODS

Chemicals and instruments:

All chemicals, reagents and solvents were of analytical grade and used directly without extra purification. Chemicals and solvents were purchased from the corresponding companies (Alfa Aesar, Acros Organics, Sigma-Aldrich, Fluka, SD fine Chem Limited, Tedia and Fisher Scientific). Melting points were measured using Gallenkamp melting point apparatus and uncorrected. Infrared (IR) spectra were recorded using Shimadzu IR affinity1 Fourier-Transform Infrared (FTIR) spectrophotometer. All samples were prepared with potassium bromide and pressed into a disc. ^{1}H-Nuclear Magnetic Resonance (NMR) and ^{13}C-NMR spectra were measured on Bruker, Avance DPX 500 and Bruker 300 MHz-Avance III spectrometers. Chemical shifts are given in δ (ppm) using Tetramethylsilane (TMS) as internal reference; the samples were dissolved in Deuterated chloroform ($CDCl_3$) or Dimethyl Sulfoxide (DMSO)-d_6. High Resolution Mass Spectrometry (HR-MS) was performed using Liquid Chromatography (LC) mass Bruker Apex-IV mass spectrometer utilizing an electrospray interface. AFLX800TBI micro plate Fluor meter was used in the *in vitro* bioassay (BioTek Instruments, Winooski, Vermont, USA).

Thin Layer Chromatography (TLC) was performed on 20×20 cm with layer thickness of 0.2 mm aluminum cards pre-coated with fluorescent silica gel GF254 DC-alufolien-kieselgel (Fluka analytical, Germany) and visualized by Ultraviolet (UV) light indicator (at 254 and/or 360 nm). Commercially available CETP inhibition drug screening kit was used (BioVision, Linda Vista Avenue, USA).

Synthesis of methyl 3-(4-(trifluoromethyl) benzylamino) benzoate intermediate (5)[51]:

3-Aminobenzoic acid (1, 2.0 g, 14.58 mmol) was dissolved in methanol (20 ml) and cooled in the ice bath. The solution was treated with oxalyl chloride (2, 2.5 ml, 29 mmol) stirred at room temperature for 20-30 min and refluxed for 24 h at 60°-70°. The reaction mixture was then evaporated and neutralized by 3 M potassium carbonate. Four times extraction by chloroform (4×20 ml) was applied. The organic layer was dried with sodium sulfate anhydrous followed by evaporation to get 2.07 g of pure 3-aminobenzoic acid methyl ester (3). Next, 3-aminobenzoic acid methyl ester (3, 2.0 g, 13.2 mmol) was dissolved in (20 ml) dichloromethane.

Addition of 1-(bromomethyl)-4-trifluoromethyl benzene (4, 3.9 ml, 25 mmol) and triethylamine (8.76 ml, 62 mmol) to the solution of 3 was done. The mixture was left under stirring at room temperature for 7 d then the mixture was evaporated. Column chromatography was carried out using cyclohexane: ethyl acetate (90:10) as eluent to afford intermediate 5: ^{1}H-NMR (DMSO-d_6, 500 MHz): δ=3.30-3.39 (m, ^{1}H, NH) 3.79 (s, 3H, OCH_3), 4.43 (d, 2H, CH_2), 6.74 (t, ^{1}H, Ar-H), 7.08 (d, J=7.80 Hz, ^{1}H, Ar-H), 7.14-7.21 (m, 2H, Ar-H), 7.58 (d, J=8.0 Hz, 2H, Ar-H), 7.69 (d, J=8.1 Hz, 2H, Ar-H) ppm; ^{13}C-NMR (DMSO-d_6, 125 MHz): δ=46.3 (1C), 52.4 (1C), 113.2 (1C), 117.0 (1C), 117.2 (1C), 123.7 (1C), 125.6 (1C), 125.7 (1C), 125.9 (1C), 128.2 (2C), 129.7 (1C), 130.8 (1C), 145.4 (1C), 149.0 (1C), 167.1 (1C) ppm; IR (KBr) νmax 3395, 3040, 2963, 2916, 1721, 1659, 1597, 1535, 1435, 1311 and 1227 cm^{-1}.

General procedure for the synthesis of the targeted compounds (8a-e):

The intermediate methyl 3-(4-(trifluoromethyl) benzylamino) benzoate (5) was dissolved in 1 M sodium hydroxide (5 ml) and refluxed overnight at 100°, then the reaction mixture was neutralized with 1 M Hydrochloric acid (HCL) and extracted three times using chloroform (3×20 ml). The organic layer was dried using anhydrous sodium sulfate and evaporated.

Subsequently, the intermediate 3-(4-(trifluoromethyl) benzylamino) benzoic acid (6, 0.31 g, 1.0 mmol) was dissolved in 10 ml dichloromethane and oxalyl chloride (2, 0.17 ml, 2.0 mmol) was added. The reaction was left under stirring for 5 d at 50°-60°. Later the reaction mixture was evaporated.

N-(4-Methoxy-benzyl)-N'-(3-(4-methoxy-benzylcarbamoyl)-phenyl)-N'-(4

trifluoromethylbenzyl)-oxalamide (8a): 4-Methoxy benzylamine (7a, 0.39 ml, 3.0 mmol) was added together with 5 ml of triethylamine and stirred at room temperature for 5 d. Then the crude product was purified by column chromatography using chloroform:methanol (98:2) as eluent to afford 8a as an off-white powder (70 %); m.p. 89°-91°; R_f=0.92 (Trichloromethane ($CHCl_3$):Methanol (MeOH), 90:10); ^{1}H-NMR (DMSO-d_6, 300 MHz): δ=3.67 (s, 6H, 2×OCH_3), 4.20-4.43 (m, 4H, 2×Methylene (CH_2)), 5.03 (s, 2H, CH_2), 6.64-6.85 (m, 6H, Ar-H), 7.09-7.29 (m, 4H, Ar-H), 7.37-7.53 (m, 3H, Ar-H), 7.57-7.72 (m, 3H, Ar-H), 8.97 (t, 1H, NH), 9.14 (t, ^{1}H, NH) ppm; ^{13}C-NMR (DMSO-d_6, 75 MHz): δ=42.6 (2C), 46.3 (1C), 55.5 (2C), 114.1 (4C), 125.8 (2C), 126.5 (1C), 126.9 (1C), 128.6 (1C), 128.7 (1C), 129.0 (4C), 130.4 (1C), 131.8 (1C), 131.9 (1C), 135.9 (1C), 139.4 (1C), 140.9 (1C), 141.4 (1C), 141.8 (1C), 158.7 (2C), 163.3 (1C), 164.1 (1C), 165.5 (1C), 165.6 (1C) ppm; IR (KBr) νmax 3534, 3287, 3071, 2932, 2916, 1666, 1589, 1543, 1412, 1327, 1250 cm^{-1}; HR-MS (Electrospray Ionization (ESI), negative mode) m/z $[M-1]^+$ 604.20670 ($C_{33}H_{29}F_3N_3O_5$ requires 604.21376).

N-(4-Methyl-benzyl)-N'-[3-(4-methyl-benzylcarbamoyl)-phenyl]-N'-(4-trifluoromethyl-benzyl) oxalamide (8b): 4-Methyl benzylamine (7b, 0.38 ml, 3.0 mmol) was added together with 5 ml of triethylamine and stirred at room temperature for 5 d. Then the crude product was purified by column chromatography using chloroform:methanol (98:2) as eluent to afford 8b as an off-white powder (20 %); m.p. 141°-143°; R_f=0.85 ($CHCl_3$:MeOH, 90:10); ^{1}H-NMR (DMSO-d_6, 500 MHz): δ=2.23 (s, 6H, 2×CH_3), 3.84 (d, 2H, CH_2), 4.08 (d, 2H, CH_2), 5.07 (s, 2H, CH_2), 6.78 (d, J=7.85 Hz, 2H, Ar-H), 6.97 (d, J=7.75 Hz, 2H, Ar-H), 7.09-7.25 (m, 3H, Ar-H), 7.45 (d, J=7.75 Hz, 4H, Ar-H), 7.55 (d, J=7.95 Hz, 2H, Ar-H), 7.59 (s, 1H, Ar-H), 7.69 (d, J=7.95 Hz, 2H, Ar-H), 8.76 (t, ^{1}H, NH), 9.23 (t, ^{1}H, NH) ppm; ^{13}C-NMR (DMSO-d_6, 125 MHz): δ=21.2 (2C), 44.3 (2C), 46.8 (1C), 125.7 (1C), 125.8 (1C), 127.1 (2C), 127.6 (2C), 128.3 (1C), 128.9 (1C), 129.2 (2C), 129.3 (2C), 130.2 (1C), 131.1 (1C), 132.7 (1C), 135.5 (1C), 136.2 (1C), 136.4 (1C), 136.5 (1C), 139.4 (1C), 141.3 (1C), 141.5 (1C), 160.6 (1C), 163.1 (1C), 163.3 (1C), 164.0 (1C), 165.5 (1C), 165.8 (1C) ppm; IR (KBr) νmax 3665, 3410, 3032, 2924, 1728, 1651, 1528, 1451, 1397, 1338, 1265 cm^{-1}; HR-MS (ESI, negative mode) m/z $[M]^+$ 573.18511 ($C_{33}H_{30}F_3N_3O_3$ requires 573.22393).

N-(3-Fluoro-benzyl)-N'-[3-(3-fluoro-benzylcarbamoyl)-phenyl]-N'-(4-trifluoromethyl-benzyl)-oxalamide (8c): 3-Fluoro benzylamine (7c, 0.34 ml, 3.0 mmol) was added together with 5 ml of triethylamine and stirred at room temperature for 5 d. Then the crude product was purified by column chromatography using chloroform:methanol (99:1) as eluent to afford 8c as an off-white powder (20 %); m.p. 111°-112°; R_f=0.54 ($CHCl_3$:MeOH, 99:1); ^{1}H-NMR (DMSO-d_6, 300 MHz): δ=4.13 (d, 2H, CH_2), 4.45 (d, 2H, CH_2), 5.05 (s, 2H, CH_2), 6.94 (d, J=9.0 Hz, 2H, Ar-H), 7.03-7.15 (m, 4H, Ar-H), 7.24-7.33 (m, 4H, Ar-H), 7.46 (d, J=9.0 Hz, 2H, Ar-H), 7.60-7.69 (m, 4H, Ar-H), 9.07 (t, ^{1}H, NH), 9.27 (t, ^{1}H, NH) ppm; ^{13}C-NMR (DMSO-d_6, 75 MHz): δ=43.6 (2C), 48.2 (1C), 113.9 (1C), 114.2 (2C), 114.5 (1C), 123.4 (1C), 123.7 (1C), 125.8 (1C), 126.7 (1C), 126.9 (1C), 128.7 (1C), 129.1 (2C), 129.6 (1C), 130.7 (2C), 130.8 (1C), 135.6 (1C), 139.0 (1C), 140.0 (1C), 140.1 (1C), 140.8 (1C), 141.9 (1C), 142.8 (1C), 164.1 (1C), 164.7 (1C), 164.9 (1C), 165.5 (1C), 165.6 (1C) ppm; IR (KBr) νmax 3325, 3078, 2963, 2924, 1651, 1605, 1543, 1451, 1327, 1258 cm^{-1}.

N-(3-Bromo-benzyl)-N'-[3-(3-bromo-benzylcarbamoyl)-phenyl]-N'-(4-trifluoromethyl-benzyl)-oxalamide (8d): 3-Bromo benzylamine (7d, 0.38 ml, 3.0 mmol) was added together with 5 ml of triethylamine and stirred at room temperature for 5 d. Then the crude product was purified by column chromatography using cyclohexane:ethyl acetate (6:4) as eluent to afford 8 d as a pale yellow viscous liquid (48 %); R_f=0.33 (cyclohexane:EtOH, 50:50); ^{1}H-NMR ($CDCl_3$, 500 MHz): δ=4.26 (d, 2H, CH_2), 4.56 (d, 2H, CH_2), 4.96 (s, 2H, CH_2), 7.05-7.08 (m, 2H, Ar-H), 7.13 (t, 3H, Ar-H), 7.30-7.35 (m, 4H, Ar-H), 7.40 (d, J=7.50 Hz, 2H, Ar-H), 7.51 (d, J=7.95 Hz, 2H, Ar-H), 7.59 (s, ^{1}H, Ar-H), 7.64 (d, J=7.65 Hz, 2H, Ar-H), 8.95 (t, ^{1}H, NH), 9.14 (t, ^{1}H, NH) ppm; ^{13}C-NMR ($CDCl_3$,125 MHz): δ=42.8 (1C), 43.6 (1C), 54.4 (1C), 122.7 (1C), 122.8 (1C), 125.0 (1C), 125.6 (1C), 125.7 (1C), 125.8 (1C), 126.1 (1C), 126.3 (2C), 126.5 (1C), 129.1 (1C), 129.5 (1C), 130.0 (1C), 130.3 (1C), 130.4 (2C), 130.7 (1C), 130.8 (1C), 130.9 (2C), 135.5 (1C), 139.2 (1C), 139.6 (1C), 140.2 (1C), 142.2 (1C), 159.8 (1C), 161.9 (1C), 166.1 (1C) ppm; IR (KBr) νmax 3330, 3063, 2963, 2909, 1651, 1543, 1412, 1327, 1265 cm^{-1}.

N-(4-Fluoro-benzyl)-N'-[3-(4-fluoro-benzylcarbamoyl)-phenyl]-N'-(4-trifluoromethyl-benzyl)-oxalamide (8e): 4-Fluoro benzylamine (7e,

0.34 ml, 3.0 mmol) was added together with 5 ml of triethylamine and stirred at room temperature for 5 d. Then the crude product was purified by column chromatography using chloroform as eluent to afford 8e as a white powder (36 %); m.p. 132.5°-133.5°; R_f=0.69 ($CHCl_3$:MeOH, 98:2); ^{1}H-NMR ($CDCl_3$, 300 MHz): δ=4.25 (d, 2H, CH_2), 4.53 (d, 2H, CH_2), 4.94 (s, 2H, CH_2), 6.98 (d, J=9.0 Hz, 4H, Ar-H), 7.01 (d, J=9.0 Hz, 2H, Ar-H), 7.24-7.35 (m, 5H, Ar-H), 7.50 (d, J=6.0 Hz, 2H, Ar-H), 7.57 (s, ^{1}H, Ar-H), 7.61 (d, J=9.0 Hz, 2H, Ar-H), 9.00 (t, ^{1}H, NH), 9.13 (t, ^{1}H, NH) ppm; ^{13}C-NMR ($CDCl_3$, 75 MHz): δ=42.7 (1C), 43.5 (1C), 54.4 (1C), 115.5 (2C), 115.8 (2C), 125.6 (1C), 125.7 (1C), 125.8 (1C), 126.0 (1C), 129.1 (2C), 129.5 (2C), 129.6 (1C), 129.7 (1C), 129.8 (1C), 130.0 (2C), 132.7 (1C), 132.8 (1C), 133.9 (1C), 135.6 (1C), 139.6 (1C), 142.3 (1C), 154.8 (1C), 160.7 (1C), 162.0 (1C), 163.9 (1C), 166.1 (1C) ppm; IR (KBr) νmax 3367, 3279, 3078, 2924, 2855, 1767, 1651, 1543, 1512, 1404, 1327, 1227 cm^{-1}.

Synthesis of methyl 3-(4-(1,1,2,2-tetrafluoroethoxy) benzylamino) benzoate intermediate (11)[47]:

3-Aminobenzoic acid (1, 2.0 g, 14.58 mmol) was dissolved in methanol (20 ml) and cooled in the ice bath. The solution was treated with oxalyl chloride (2, 2.5 ml, 29 mmol), stirred at room temperature for 20-30 min and refluxed for 24 h at 60°-70°. Evaporation of the reaction mixture followed by neutralization using 3 M potassium carbonate was carried out. Extraction by chloroform (5×20 ml) was applied. Then the organic layer was dried with sodium sulfate anhydrous followed by evaporation to obtain 2.05 g of pure 3-aminobenzoic acid methyl ester (3).

Next, 3-aminobenzoic acid methyl ester (3, 2.0 g, 13.2 mmol) was dissolved in (20 ml) Dimethylformamide (DMF) and 4-(1,1,2,2-tetrafluoroethoxy) benzaldehyde (9, 4.85 ml, 22 mmol) was added. The mixture was refluxed at 100°-140° for 7 d after the addition of 2 drops of HCL. Evaporation of the mixture followed by purification by column chromatography using cyclohexane:ethyl acetate (8:2) as eluent to attain the intermediate methyl 3-(4-(1,1,2,2-tetrafluoroethoxy) benzylideneamino) benzoate (10). Afterward, methyl 3-(4-(1,1,2,2-tetrafluoroethoxy) benzylideneamino) benzoate (10, 3.6 g, 13 mmol) was dissolved in (20 ml) methanol, then gradual addition of Sodium borohydride ($NaBH_4$) (2.46 g, 65 mmol) was carried out. The mixture was stirred at room temperature for 3 d. Subsequently, the mixture was evaporated and the intermediate methyl 3-(4-(1,1,2,2-tetrafluoroethoxy) benzylamino) benzoate (11) was purified by column chromatography using cyclohexane:ethyl acetate (9.7:0.3) as eluent; ^{1}H-NMR (DMSO-d_6, 500 MHz): δ=3.25-3.54 (m, ^{1}H, NH), 3.73 (s, 3H, OCH_3), 4.56 (d, 2H, CH_2), 6.66 (d, J=8.65 Hz, 2H, Ar-H), 7.19-7.31 (m, ^{1}H, CF_2H), 7.67 (d, J=8.60 Hz, 2H, Ar-H), 7.97 (s, ^{1}H, Ar-H), 8.06-8.12 (m, 3H, Ar-H) ppm; IR (KBr) νmax 3379, 1705, 1612, 1512, 1442, 1350, 1200 cm^{-1}.

General procedure for the synthesis of the targeted compounds (8f-j):

The intermediate 11 was dissolved in 1 M sodium hydroxide (5 ml) and refluxed overnight at 100°, then the reaction mixture was neutralized with 1 M HCL and extracted three times using chloroform (3×20 ml). The organic layer was dried using anhydrous sodium sulfate and evaporated to obtain intermediate 3-(4-(1,1,2,2-tetrafluoroethoxy) benzylamino) benzoic acid (12).

Subsequently, the intermediate 12 (0.31 g, 1.0 mmol) was dissolved in 10 ml dichloromethane and oxalyl chloride (2, 0.17 ml, 2.0 mmol) was added. The reaction was left under stirring for 5 d at 50°-60°. Later the reaction mixture was evaporated.

N-(4-Methoxy-benzyl)-N'-[3-(4-methoxy-benzylcarbamoyl)-phenyl]-N'-[4-(1,1,2,2-tetrafluoro-ethoxy)-benzyl]-oxalamide (8f): 4-Methoxy benzylamine (7a, 0.39 ml, 3.0 mmol) was added together with 5 ml of triethylamine and stirred at room temperature for 5 d. Then the crude product was purified by column chromatography using chloroform:methanol (98:2) as eluent to afford 8f as a pale yellow liquid (15 %); R_f=0.75 ($CHCl_3$:MeOH, 97:3); ^{1}H-NMR (DMSO-d_6, 500 MHz): δ=3.72 (s, 3H, OCH_3), 3.73 (s, 3H, OCH_3), 4.01 (d, 2H, CH_2), 4.41 (d, 2H, CH_2), 5.00 (s, 2H, CH_2), 6.68 (t, ^{1}H, CF_2H), 6.77 (d, J=8.55 Hz, 2H, Ar-H), 6.81 (d, J=8.45 Hz, 2H, Ar-H), 6.89 (d, J=8.45 Hz, 2H, Ar-H), 7.21-7.28 (m, 6H, Ar-H), 7.34 (d, J=8.10 Hz, 2H, Ar-H), 7.82-7.85 (m, 2H, Ar-H), 8.98 (t, ^{1}H, NH), 9.14 (t, ^{1}H, NH) ppm; ^{13}C-NMR (DMSO-d_6, 125 MHz): δ=41.4 (1C), 42.6 (1C), 51.0 (1C), 55.4 (2C), 114.1 (2C), 114.2 (4C), 121.9 (2C), 126.6 (1C), 126.8 (1C), 128.8 (2C), 129.1 (4C), 130.1 (2C), 130.4 (1C), 130.6 (1C), 131.9 (1C), 135.8 (1C), 140.9 (1C), 147.7 (1C), 158.6 (1C), 158.7 (1C), 163.3 (1C), 165.4 (1C), 165.5 (1C) ppm; IR (KBr) νmax 3318, 3071, 2963, 1659, 1582, 1543, 1404, 1327 cm^{-1}.

N-(4-Methyl-benzyl)-N'-[3-(4-methyl-benzylcarbamoyl)-phenyl]-N'-[4-(1,1,2,2-tetrafluoro-ethoxy)-benzyl]-oxalamide (8g): 4-Methyl benzylamine (7b, 0.38 ml, 3.0 mmol) was added together with 5 ml of triethylamine and stirred at room temperature for 5 d. Then the crude product was purified by column chromatography using chloroform:methanol (98:2) as eluent to afford 8 g as an off white powder (33.3 %); decomposes above 300°; R_f=0.73 ($CHCl_3$:MeOH, 98:2); ^{1}H-NMR (DMSO-d_6, 300 MHz): δ=2.22 (s, 3H, CH_3), 2.46 (s, 3H, CH_3), 3.90-4.09 (m, 2H, CH_2), 4.34-4.45 (m, 2H, CH_2), 4.67 (s, 2H, CH_2), 6.50-6.51 (m, ^{1}H, CF_2H), 6.65-6.78 (m, 2H, Ar-H), 6.79-6.86 (m, ^{1}H, Ar-H), 6.88-7.00 (m, 3H, Ar-H), 7.08-7.21 (m, 4H, Ar-H), 7.23-7.45 (m, 3H, Ar-H), 7.74-7.88 (m, 3H, Ar-H), 8.96 (t, ^{1}H, NH), 9.12 (t, ^{1}H, NH) ppm; ^{13}C-NMR (DMSO-d_6, 75 MHz): δ=21.1 (2C), 41.9 (1C), 42.9 (2C), 121.9 (1C), 122.0 (2C), 126.7 (1C), 126.8 (1C), 127.5 (2C), 127.7 (2C), 129.2 (1C), 129.3 (4C), 129.8 (1C), 130.2 (2C),130.4 (1C), 135.0 (1C), 135.8 (1C), 136.3 (1C), 136.9 (1C), 139.2 (1C), 140.9 (1C), 147.6 (1C), 163.1 (1C), 164.0 (1C), 165.5 (2C) ppm; IR (KBr) νmax 3318, 3063, 2924, 1651, 1543, 1512, 1435, 1303, 1196 cm^{-1}; HR-MS (ESI, positive mode) m/z $[M+Na]^+$ 644.21271 ($C_{34}H_{32}F_4N_3O_4Na$ requires 644.22507).

N-(3-Fluoro-benzyl)-N'-[3-(3-fluoro-benzylcarbamoyl)-phenyl]-N'-[4-(1,1,2,2-tetrafluoro-ethoxy)-benzyl]-oxalamide (8h): 3-Fluoro benzylamine (7c, 0.34 ml, 3.0 mmol) was added together with 5 ml of triethylamine and stirred at room temperature for 5 d. Then the crude product was purified by column chromatography using chloroform:methanol (97:3) as eluent to afford 8 h as a yellow viscous liquid (14.6 %); R_f=0.30 ($CHCl_3$:MeOH, 98:2); ^{1}H-NMR ($CDCl_3$, 300 MHz): δ=4.25 (d, 2H, CH_2), 4.55 (d, 2H, CH_2), 4.89 (s, 2H, CH_2), 5.87 (t, 1H, CF_2H), 6.43-6.51 (m, 2H, Ar-H), 6.81 (d, J=9.0 Hz, 2H, Ar-H), 6.94 (t, J=6.0 Hz, 2H, Ar-H), 7.06-7.10 (m, 3H, Ar-H), 7.17-7.23 (m, 2H, Ar-H), 7.51-7.54 (m, 3H, Ar-H), 7.64 (d, J=9.0 Hz, 2H, Ar-H), 8.93 (t, ^{1}H, NH), 9.23 (t, ^{1}H, NH) ppm; ^{13}C-NMR ($CDCl_3$, 75 MHz): δ=42.8 (1C), 43.7 (1C), 54.0 (1C), 114.4 (1C), 114.5 (1C), 114.6 (1C), 114.9 (1C), 121.8 (2C), 123.2 (1C), 123.4 (1C), 125.9 (1C), 126.2 (1C), 129.4 (1C), 130.3 (2C), 130.4 (2C), 130.5 (1C), 134.0 (1C), 135.5 (1C), 139.5 (1C), 139.6 (1C), 140.6 (1C), 140.7 (1C), 142.1 (1C), 148.5 (1C), 160.0 (1C), 161.3 (1C), 162.0 (1C), 164.8 (1C), 166.2 (1C) ppm; IR (KBr) νmax 3372, 3240, 3086, 2916, 2847, 1690, 1636, 1589, 1481, 1427, 1397, 1304, 1273 cm^{-1}.

N-(3-Bromo-benzyl)-N'-[3-(3-bromo-benzylcarbamoyl)-phenyl]-N'-[4-(1,1,2,2-tetrafluoro-ethoxy)-benzyl]-oxalamide (8i): 3-Bromo benzylamine (7 d, 0.38 ml, 3.0 mmol) was added together with 5 ml of triethylamine and stirred at room temperature for 5 d. Then the crude product was purified by column chromatography using chloroform:methanol (99.5:0.5) as eluent to afford 8i as a yellow liquid (17 %); R_f=0.58 ($CHCl_3$:MeOH, 95:5); ^{1}H-NMR (DMSO-d_6, 500 MHz): δ=4.31 (d, 2H, CH_2), 4.48 (d, 2H, CH_2), 4.83 (s, 2H, CH_2), 6.51-6.52 (m, ^{1}H, CF2H), 7.27-7.34 (m, 4H, Ar-H), 7.37-7.40 (m, 3H, Ar-H), 7.45-7.49 (m, 3H, Ar-H), 7.61-7.65 (m, 2H, Ar-H), 7.67-7.72 (m, 4H, Ar-H), 8.97 (t, ^{1}H, NH), 9.16 (t, ^{1}H, NH) ppm; ^{13}C-NMR (DMSO-d_6, 125 MHz): δ=41.3 (1C), 41.4 (1C), 44.4 (1C), 121.8 (1C), 121.9 (1C), 122.1 (2C), 123.4 (1C), 123.6 (1C), 123.7 (1C), 125.1 (1C), 125.7 (1C), 125.8 (1C), 126.6 (1C), 126.8 (2C), 130.2 (2C), 130.4 (2C), 130.9 (2C), 131.1 (2C), 134.9 (1C), 139.1 (1C), 142.4 (2C), 143.0 (1C), 161.7 (2C), 165.5 (1C) ppm; IR (KBr) νmax 3526, 3264, 3048, 2924, 2855, 1667, 1528, 1435, 1389, 1258 cm-1.

N-(4-Fluoro-benzyl)-N'-[3-(4-fluoro-benzylcarbamoyl)-phenyl]-N'-[4-(1,1,2,2-tetrafluoro-ethoxy)-benzyl]-oxalamide (8j): 4-Fluoro benzylamine (7e, 0.34 ml, 3.0 mmol) was added together with 5 ml of triethylamine and stirred at room temperature for 5 d. Then the crude product was purified by column chromatography using chloroform:ethyl acetate (99:1) as eluent to afford 8j as a white powder (45 %); m.p. 128°-129°; R_f=0.60 ($CHCl_3$:MeOH, 98:2); ^{1}H-NMR (DMSO-d_6, 300 MHz): δ=4.34 (d, 2H, CH_2), 4.41 (d, 2H, CH_2), 4.67 (s, 2H, CH_2), 6.72 (t, ^{1}H, CF2H), 6.84 (d, J=9.0 Hz, 4H, Ar-H), 7.02 (d, J=9.0 Hz, 4H, Ar-H), 7.10 (d, J=9.0 Hz, 2H, Ar-H), 7.26-7.35 (m, 2H, Ar-H), 7.38-7.43 (m, 2H, Ar-H), 7.89 (d, J=9.0 Hz, 2H, Ar-H), 8.98 (t, ^{1}H, NH), 9.09 (t, ^{1}H, NH) ppm; ^{13}C-NMR (DMSO-d_6, 75 MHz): δ=42.5 (2C), 48.5 (1C), 115.3 (2C), 115.6 (2C), 121.9 (2C), 122.1 (2C), 122.3 (1C), 127.4 (1C), 127.5 (1C), 129.5 (2C), 129.7 (2C), 129.8 (2C), 131.1 (1C), 135.4 (1C), 135.6 (1C), 136.0 (1C), 136.1 (1C), 139.4 (1C), 147.6 (1C), 163.4 (1C), 164.0 (2C), 165.4 (2C) ppm; IR (KBr) νmax 3364, 3279, 3078, 2924, 2855, 1767, 1651, 1543, 1512, 1404, 1327 cm^{-1}.

Modeling methods:

CETP structure preparation: CETP coordinates (Protein Data Bank (PDB) ID: 4EWS)[38] were adopted from the Research Collaboratory for Structural Bioinformatics (RCSB) PDB. They were energetically minimized using protein preparation module in the Schrödinger software to optimize H-bond interactions[52].

Ligand structures preparation: Targeted compounds were built recruiting the co-crystallized ligand's (0RP) coordinates as a template in 4EWS[38]. MAESTRO Build panel was used to build ligands then they were energetically minimized by MacroModel program[52] using OPLS2005 force field.

Glide docking: Glide grid generation module was used to produce the Grid file for CETP[52] recognizing the bound ligand as centroid. Van der Waals scaling factor of the nonpolar atoms was calibrated to 0.8 while other parameters were set as defaults. The binding affinity represents docking score (Kcal/mol).

Pharmacophore mapping: The synthesized compounds 8a-j were mapped against an adopted pharmacophore model of CETP inhibitors[47].

CETP inhibition bioassay: The CETP inhibitory activity of the synthesized compounds and torcetrapib inhibitor was evaluated *in vitro* according to the procedure used earlier[49].

RESULTS AND DISSCUSION

A series of benzyloxalamides 8a-j were synthesized as shown in fig. 1. The synthesis started with the activation of the carboxylic acid moiety of 3-aminobenzoic acid using oxalyl chloride in the presence of methanol to produce the corresponding methyl ester protecting group. Next, the amine nitrogen of 3-amino benzoic acid methyl ester attacked the partially positive methylene group of the benzyl bromide in the presence of DCM as a solvent to produce substituted 3-benzylaminobenzoic acid methyl ester intermediate. Triethylamine was used as an acid scavenger[49].

On the other hand, formation of imine 10 was attained by the nucleophile attack of the amine nitrogen of 3-aminobenzoic acid methyl ester on the partially positive carbonyl carbon of the 4-(1,1,2,2-tetrafluoroethoxy) benzaldehyde followed by the elimination of a molecule of water resulting in the acid-catalyzed formation of intermediate. Afterward, reduction of the imine intermediate was carried out by $NaBH_4$ where a hydride ion attacks the electrophilic carbon of the imine functional group (C=N) and the anion that forms is then protonated to generate the secondary amine using methanol as a solvent at room temperature for 3 d[47].

Afterward, deprotection of the carboxylic acid group of 3-aminobenzoic acid methyl ester intermediates was carried out by alkaline hydrolysis using 1 M

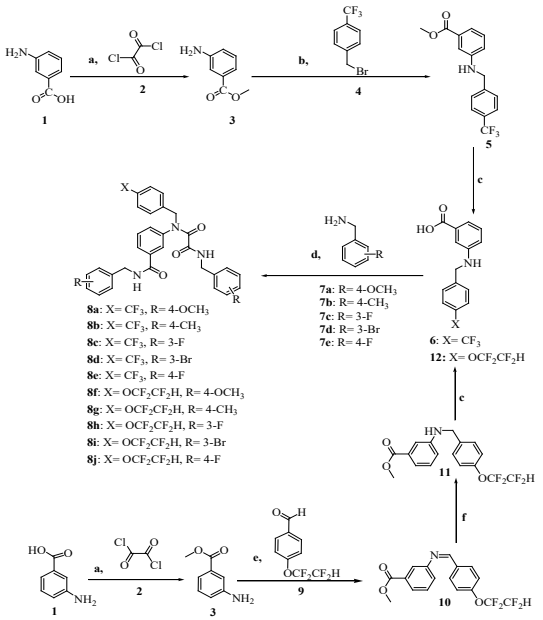

Fig. 1: Synthesis of fluorinated benzyloxalamide derivatives 8a-j. Reagents and conditions, (a): CH_3OH/reflux (60°-70°), 24 h; (b): DCM, TEA, RT, 5 d; (c): 1 M NaOH (100°), overnight and 1M HCl; (d): $(COCl)_2$, TEA, DCM, RT, 5 d; (e) DMF/reflux (100°-140°), 7 d/HCl after 24 h and (f): CH_3OH, $NaBH_4$, RT, 3 d

NaOH under reflux followed by neutralization with 1 M HCL. Again, activation of the carboxylic acid moiety of 3-benzylamino benzoic acid intermediates was performed using oxalyl chloride to produce the corresponding acyl chloride derivatives in the presence of triethylamine and DCM. Additionally, oxalyl chloride reacted with the amine moiety of 3-benzylamino benzoic acid intermediates. Subsequently, amide formation was attained by the nucleophile attack of the amine moiety of benzylamine (7a-e) on the partially positive carbonyl carbon of the previously produced benzoyl chloride and acyl chloride to get the targeted benzyloxalamides 8a-j. The best yield was obtained upon reacting intermediate 6 with 4-methoxy benzylamine (7a) to produce 8a in 70 % yield.

The results of CETP inhibition bioassay, presented in Table 1, demonstrate that most of the synthesized benzamides 8a-j has appreciable CETP inhibitory activity with the compound 8f exhibiting promising activity against CETP with a percent inhibition of 64.1 % at 10 µM concentrations and an half-maximal Inhibitory Concentration (IC_{50}) of 2.1 µM.

Structure activity relationship study of the synthesized compounds 8a-j reveals that (fig. 1 and Table 1) the presence of p-tetrafluoroethoxy group (as in compounds 8f-8j) gives greater inhibitory activity than the p-trifluoromethyl group (as in compounds 8a-8e) regardless of the lipophilic and electronic properties of the substituent R group. Furthermore, it looks that the m-R substituent (as in compounds 8c, 8d, 8h and 8i) decreases the CETP inhibitory activity of the synthesized compounds when compared to the p-substituted analogues (as in compounds 8a, 8e, 8f, 8g and 8j).

With the aim of determining the binding basis of the co-crystallized ligand (0RP: torcetrapib) and synthesized compounds 8a-j in CETP binding domain (PDB ID: 4EWS), Glide docking protocol[53,54] was applied against 4EWS. Glide docking results show that the verified compounds accommodate the active site of CETP. Fig. 2 shows that the docked pose of 8f overlaid the conformation of 0RP.

It's worth noting that the series exhibit comparable binding affinity to that of 0RP. Hydrophobic interaction presides ligand/4EWS complex formation as shown in Table 2, fig. 3 and fig. 4.

TABLE 1: *IN VITRO* CETP INHIBITORY BIOACTIVITIES OF THE TARGETED BENZYLOXALAMIDES

Compound	X	R	% Inhibition	IC_{50} (µM)
8a	CF_3	4-OCH_3	24.0[a]	-----
8b	CF_3	4-CH_3	0.0[a]	-----
8c	CF_3	3-F	12.3[a]	-----
8d	CF_3	3-Br	13.7[a]	-----
8e	CF_3	4-F	36.3[a]	-----
8f	OCF_2CF_2H	4-OCH_3	64.1[a]	2.1 (R^2=0.99)
8g	OCF_2CF_2H	4-CH_3	36.4[a]	-----
8h	OCF_2CF_2H	3-F	17.0[a]	-----
8i	OCF_2CF_2H	3-Br	27.1[a]	-----
8j	OCF_2CF_2H	4-F	40.1[a]	-----
Torcetrapib	-	-	82.2[b]	0.04

Note: a: Tested at 10 µM concentration, b: Tested at 0.08 µM concentration

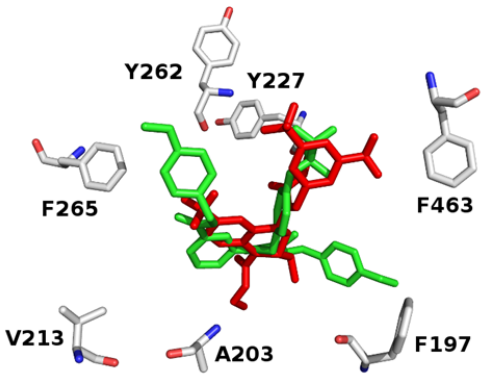

Fig. 2: Overlaying of the Glide docked pose of 8f (represented in green color) and the co-crystallized ligand (red color)

TABLE 2: GLIDE DOCKING SCORES OF THE TARGETED COMPOUNDS

Compound	Glide docking scores (Kcal/mol)	H-Bond
8a	-11.53	NA
8b	-11.54	NA
8c	-10.4	NA
8d	-12.75	NA
8e	-12.14	NA
8f	-11.49	NA
8g	-12.45	NA
8h	-11.97	NA
8i	-13.13	NA
8j	-12.76	NA
Torcetrapib (0RP)	-10.57	NA

Note: NA: Not Available

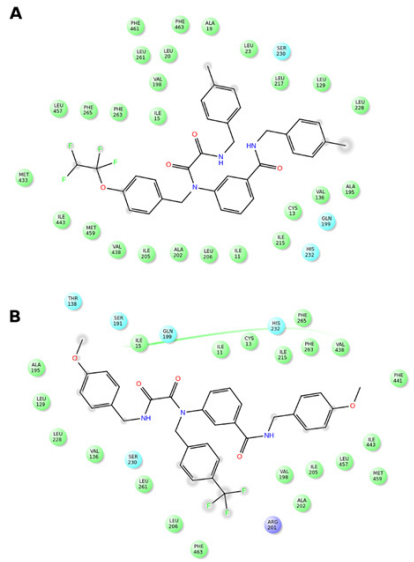

Fig. 3: The ligand/protein complex of (A): 8g and (B): 8a
Note: Hydrophobic residues are represented in green color

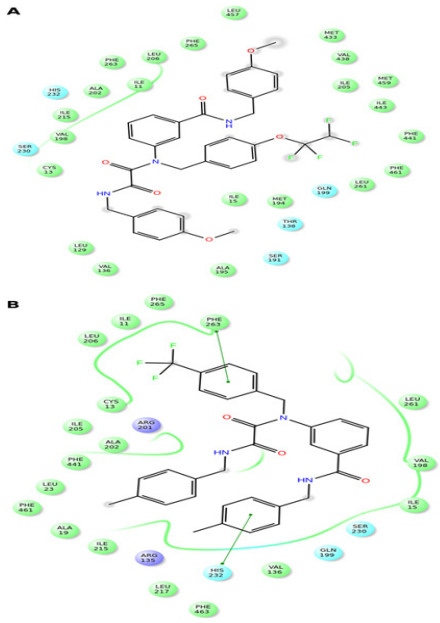

Fig. 4: The ligand/protein complex of (A): 8f and (B): 8b
Note: Hydrophobic backbone is depicted in green color

The series exhibits high binding affinity toward 4EWS as shown in their docking scores. The more the negative the docking score the higher binding affinity and better binder. In addition, a difference 2 Kcal/mol in the docking score of the co-crystallized ligand (0RP:torcetrapib) and 8g, 8i, 8j and 8d indicates that the core structure of this series might be promising scaffold for CETP inhibition.

The *in vitro* biological data demonstrate that compound 8f tailored with p-OCH_3 and p-OCF_2CHF_2 moieties exerted promising CETP inhibition; implying that H-bond acceptor mediates ligand/CETP complex formation. Contrarily, swapping p-OCH_3 with p-CH_3 exemplifying by 8 g reduces the activity confirming that H-bond acceptor is essential for binding interaction. However, the comparable activity of 8j to that of 8g interrogates that para H-bond acceptor accompanies with small hydrophobic motif illustrated with p-OCH3 potentiates the activity. Moreover, the activity of m-F (8h) and m-Br (8i) suggests that m-substituent might impede ligand/CETP complex formation and consequently decreases the activity. Comparing the activity of 8a to that of 8f infers that p-OCF_2CHF_2 motif mediates H-bond acceptor and its length might push the ligand deeply in the binding pocket thus increases the activity.

Distinctly, the absence of activity for 8b implies that aromatic ring tailored with p-CH_3 and/or p-CF_3 decreases the activity. Furthermore, the comparable activity of 8d and 8e accords with those of 8i and 8j and confirms that m-substituent weakens the activity.

Compounds 8a-j were mapped against an adopted CETP inhibitors pharmacophore model[47]. It was found that the scaffold and its attachment moieties (8a-j) match CETP inhibitors binding groups (fig. 5)[55] and this discusses their affinity toward CETP active domain. Additionally, 8a-j occupy CETP active binding domain thus providing an explanation to their inhibitory activity.

In conclusion, ten novel fluorinated benzyloxalamides were successfully synthesized, characterized, molecular modeling studied and biologically evaluated. Targeted compound 8f was found to present a worthy lead compound for CETP inhibitors with an IC_{50} of 2.1 µM. Benzyloxalamides can serve as an encouraging new group of CETP inhibitors that can be further optimized to improve their inhibitory activity against CETP.

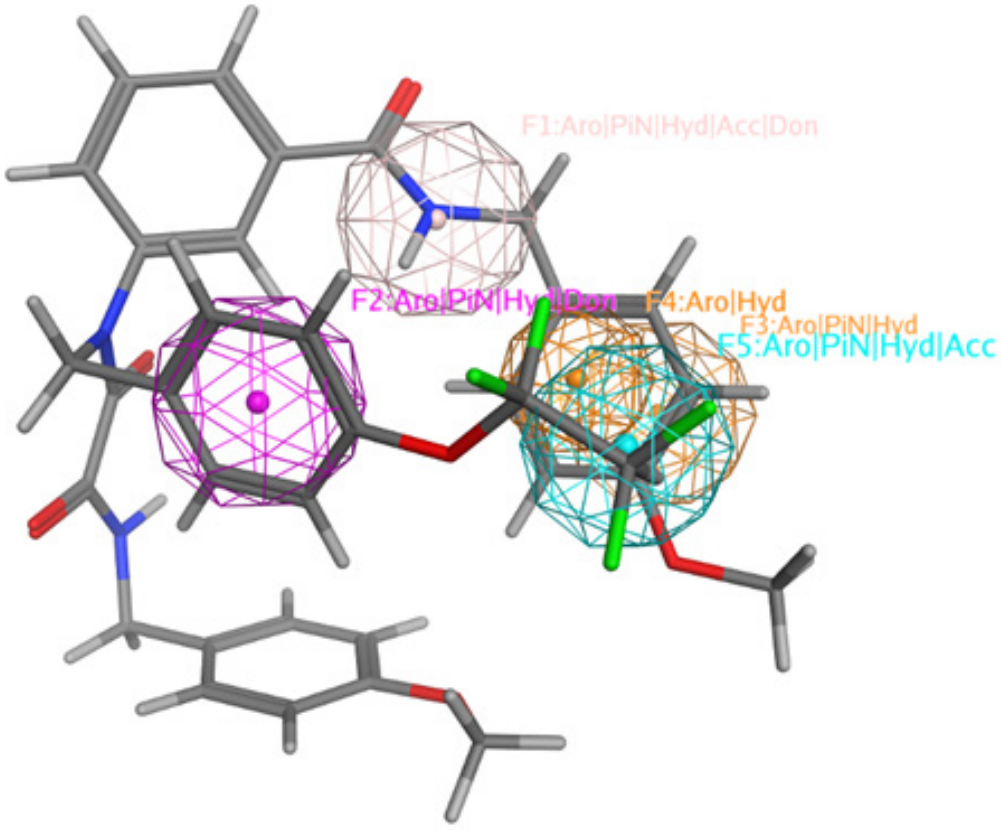

Fig. 5: CETP inhibitor pharmacophore model with 8f
Note: Aro: Aromatic rings; Acc: H-bond acceptor; Don: H-bond donor; Cat: Cationic group; PiN: π-ring and Hyd: Hydrophobic groups

Acknowledgments:

The authors acknowledge the Scientific Research at Al-Zaytoonah University of Jordan for sponsoring this project (Grant Number 20/23/2019-2020).

Conflict of interests:

The authors declared no conflict of interests.

REFERENCES

1. Sacks FM, Lichtenstein AH, Wu JH, Appel LJ, Creager MA, Kris-Etherton PM, *et al.* Dietary fats and cardiovascular disease: A presidential advisory from the American heart association. Circulation 2017;136(3):e1-23.
2. Assessment RE. Emerging risk factors collaboration. Major lipids, apolipoproteins and risk of vascular disease. JAMA 2009;302(18):1993-2000.
3. Heidenreich PA, Trogdon JG, Khavjou OA, Butler J, Dracup K, Ezekowitz MD, *et al.* Forecasting the future of cardiovascular disease in the united states: A policy statement from the American heart association. Circulation 2011;123(8):933-44.
4. Bustami J, Sukiasyan A, Kupcinskas J, Skieceviciene J, Iakoubov L, Szwed M, *et al.* Cholesteryl ester transfer protein (CETP) I405V polymorphism and cardiovascular disease in eastern European Caucasians–A cross-sectional study. BMC Geriatr 2016;16(1):144-9.
5. Karr S. Epidemiology and management of hyperlipidemia. Am J Manag Care 2017;23(9):S139-48.
6. Purva A, Sharma K, Khan MS. A review on dyslipidemia: Types, risk factors and management. Asian J Pharm Res Dev 2020;8(2):96-8.
7. Shim JS, Heo JE, Kim HC. Factors associated with dietary adherence to the guidelines for prevention and treatment of hypertension among Korean adults with and without hypertension. Clin Hyperten 2020;26(1):1-11.
8. Jarab AS, Alefishat EA, Al-Qerem W, Mukattash TL, Al-Hajjeh DA. Lipid control and its associated factors among patients with dyslipidaemia in Jordan. Int J Clin Prac 2021;75(5):e14000.
9. Ingelsson E, Schaefer EJ, Contois JH, McNamara JR, Sullivan L, Keyes MJ, *et al.* Clinical utility of different lipid measures for prediction of coronary heart disease in men and women. JAMA 2007;298(7):776-85.
10. Singh IM, Shishehbor MH, Ansell BJ. High-density lipoprotein as a therapeutic target: A systematic review. JAMA 2007;298(7):786-98.
11. Feig JE, Hewing B, Smith JD, Hazen SL, Fisher EA. High-density lipoprotein and atherosclerosis regression: Evidence from preclinical and clinical studies. Circ Res 2014;114(1):205-13.
12. Ranalletta M, Bierilo KK, Chen Y, Milot D, Chen Q, Tung E, *et al.* Biochemical characterization of cholesteryl ester transfer protein inhibitors. J Lipid Res 2010;51(9):2739-52.
13. Niesor EJ, Magg C, Ogawa N, Okamoto H, von der Mark E, Matile H, *et al.* Modulating cholesteryl ester transfer protein activity maintains efficient pre-β-HDL formation and increases reverse cholesterol transport. J Lipid Res 2010;51(12):3443-54.
14. Wang F, Kohan AB, Lo CM, Liu M, Howles P, Tso P. Apolipoprotein A-IV: A protein intimately involved in metabolism. J Lipid Res 2015;56(8):1403-18.
15. Wu BJ, Shrestha S, Ong KL, Johns D, Hou L, Barter PJ, *et al.* Cholesteryl ester transfer protein inhibition enhances endothelial repair and improves endothelial function in the rabbit. Arteriosclerosis Thromb Vasc Biol 2015;35(3):628-36.
16. Li X, Xu M, Wang F, Kohan AB, Haas MK, Yang Q, *et al.* Apolipoprotein A-IV reduces hepatic gluconeogenesis through nuclear receptor NR1D1. J Biol Chem 2014;289(4):2396-404.
17. Wang F, Kohan AB, Kindel TL, Corbin KL, Nunemaker CS, Obici S, *et al.* Apolipoprotein A-IV improves glucose homeostasis by enhancing insulin secretion. Proc Natl Acad Sci 2012;109(24):9641-6.
18. DeGoma EM, degoma RL, Rader DJ. Beyond high-density lipoprotein cholesterol levels: Evaluating high-density lipoprotein function as influenced by novel therapeutic approaches. J Am Coll Cardiol 2008;51(23):2199-211.
19. Barter PJ. Hugh sinclair lecture: The regulation and remodelling of HDL by plasma factors. Atheroscler Suppl 2002;3(4):39-47.
20. Gao S, Wang X, Cheng D, Li J, Li L, Ran L, *et al.* Overexpression of cholesteryl ester transfer protein increases macrophage-derived foam cell accumulation in atherosclerotic lesions of transgenic rabbits. Mediators Inflamm 2017;2017.
21. Gurfinkel R, Joy TR. Anacetrapib: Hope for CETP inhibitors? Cardiovasc Ther 2011;29(5):327-39.
22. Nomura A, Won HH, Khera AV, Takeuchi F, Ito K, McCarthy S, *et al.* Protein-truncating variants at the cholesteryl ester transfer protein gene and risk for coronary heart disease. Circ Res 2017;121(1):81-8.
23. Millwood IY, Bennett DA, Holmes MV, Boxall R, Guo Y, Bian Z, *et al.* Association of CETP gene variants with risk for vascular and nonvascular diseases among Chinese adults. JAMA Cardiol 2018;3(1):34-43.
24. Qiu X, Mistry A, Ammirati MJ, Chrunyk BA, Clark RW, Cong Y, *et al.* Crystal structure of cholesteryl ester transfer protein reveals a long tunnel and four bound lipid molecules. Nat Struct Mol Biol 2007;14(2):106-13.
25. Maugeais C, Perez A, von der Mark E, Magg C, Pflieger P, Niesor EJ. Evidence for a role of CETP in HDL remodeling and cholesterol efflux: Role of cysteine 13 of CETP. Biochim Biophys Acta 2013;1831(11):1644-50.
26. Benton MC, Johnstone A, Eccles D, Harmon B, Hayes MT, Lea RA, *et al.* An analysis of DNA methylation in human adipose tissue reveals differential modification of obesity genes before and after gastric bypass and weight loss. Genome Biol 2015;16(1):1-21.
27. Mabuchi H, Nohara A, Inazu A. Cholesteryl ester transfer protein (CETP) deficiency and CETP inhibitors. Mol Cells 2014;37(11):777.
28. Weers PM, Ryan RO. Apolipophorin III: Role model apolipoprotein. Insect Biochem Mol Biol 2006;36(4):231-40.
29. Barter PJ, Caulfield M, Eriksson M, Grundy SM, Kastelein JJ, Komajda M, *et al.* Effects of torcetrapib in patients at high risk for coronary events. New Engl J Med 2007;357(21):2109-22.
30. Schwartz GG, Olsson AG, Abt M, Ballantyne CM, Barter PJ, Brumm J, *et al.* Effects of dalcetrapib in patients with a recent acute coronary syndrome. New Engl J Med 2012;367(22):2089-99.
31. Lincoff AM, Nicholls SJ, Riesmeyer JS, Barter PJ, Brewer HB, Fox KA, *et al.* Evacetrapib and cardiovascular outcomes in high-risk vascular disease. New Engl J Med 2017;376(20):1933-42.
32. Rosenson RS, Brewer HB, Barter PJ, Björkegren JL, Chapman

MJ, Gaudet D, *et al.* HDL and atherosclerotic cardiovascular disease: Genetic insights into complex biology. Nat Rev Cardiol 2018;15(1):9-19.
33. Millar JS, Reyes-Soffer G, Jumes P, Dunbar RL, deGoma EM, Baer AL, *et al.* Anacetrapib lowers LDL by increasing ApoB clearance in mildly hypercholesterolemic subjects. J Clin Invest 2015;125(6):2510-22.
34. Thomas T, Zhou H, Karmally W, Ramakrishnan R, Holleran S, Liu Y, *et al.* CETP (cholesteryl ester transfer protein) inhibition with anacetrapib decreases production of lipoprotein (a) in mildly hypercholesterolemic subjects. Arteriosclerosis Thromb Vasc Biol 2017;37(9):1770-5.
35. Millar JS, Lassman ME, Thomas T, Ramakrishnan R, Jumes P, Dunbar RL, *et al.* Effects of CETP inhibition with anacetrapib on metabolism of VLDL-TG and plasma apolipoproteins C-II, C-III and E. J Lipid Res 2017;58(6):1214-20.
36. Weber O, Willmann S, Bischoff H, Li V, Vakalopoulos A, Lustig K, *et al.* Prediction of a potentially effective dose in humans for BAY 60–5521, a potent inhibitor of cholesteryl ester transfer protein (CETP) by allometric species scaling and combined pharmacodynamic and physiologically-based pharmacokinetic modelling. Br J Clin Pharmacol 2012;73(2):219-31.
37. Sarich TC, Connelly MA, Schranz DB, Ghosh A, Manitpisitkul P, Leary ET, *et al.* Phase 0 study of the inhibition of cholesteryl ester transfer protein activity by JNJ-28545595 in plasma from normolipidemic and dyslipidemic humans. Int J Clin Pharmacol Ther 2012;50(8):584-94.
38. Liu S, Mistry A, Reynolds JM, Lloyd DB, Griffor MC, Perry DA, *et al.* Crystal structures of cholesteryl ester transfer protein in complex with inhibitors. J Biol Chem 2012;287(44):37321-9.
39. Nurmohamed NS, Ditmarsch M, Kastelein JJ. CETP-inhibitors: From HDL-C to LDL-C lowering agents? Cardiovasc Res 2021;18(14):2919-31.
40. Rohman A, Arifah FH, Alam G, Rafi M. A review on phytochemical constituents, role on metabolic diseases and toxicological assessments of underutilized part of *Garcinia mangostana* L. fruit. J Appl Pharm Sci 2020;10(7):127-46.
41. Wang Y, Zhang L, Wang F, Li ZH, Dong ZJ, Liu JK. New diterpenes from cultures of the fungus *Engleromyces goetzii* and their CETP inhibitory activity. Nat Prod Bioprospect 2015;5(2):69-75.
42. Javandoost A, Afshari A, Nikbakht-Jam I, Khademi M, Eslami S, Nosrati M, *et al.* Effect of crocin, a carotenoid from saffron, on plasma cholesteryl ester transfer protein and lipid profile in subjects with metabolic syndrome: A double blind randomized clinical trial. ARYA Atheroscler 2017;13(5):245.
43. Ghaffari S, Roshanravan N. Saffron; An updated review on biological properties with special focus on cardiovascular effects. Biomed Pharmacother 2019;109:21-7.
44. Khalaf RA, Sheikha GA, Bustanji Y, Taha MO. Discovery of new cholesteryl ester transfer protein inhibitors *via* ligand-based pharmacophore modeling and QSAR analysis followed by synthetic exploration. Eur J Med Chem 2010;45(4):1598-617.
45. Sheikha GA, Khalaf RA, Melhem A, Albadawi G. Design, synthesis and biological evaluation of benzylamino-methanone based cholesteryl ester transfer protein inhibitors. Molecules 2010;15(8):5721-33.
46. Abu Khalaf R, Abu Sheikha G, Al-Sha'er M, Albadawi G, Taha M. Design, synthesis and biological evaluation of sulfonic acid ester and benzenesulfonamide derivatives as potential CETP inhibitors. Med Chem Res 2012;21(11):3669-80.
47. Abu Khalaf R, Al-Rawashdeh S, Sabbah D, Abu Sheikha G. Molecular docking and pharmacophore modeling studies of fluorinated benzamides as potential CETP inhibitors. Med Chem 2017;13(3):239-53.
48. Abu Khalaf R, Abd El-Aziz H, Sabbah D, Albadawi G, Abu Sheikha G. CETP inhibitory activity of chlorobenzyl benzamides: QPLD docking, pharmacophore mapping and synthesis. Lett Drug Des Discov 2017;14(12):1391-400.
49. Abu Khalaf R, Sabbah D, Al-Shalabi E, Bishtawi S, Albadawi G, Abu Sheikha G. Synthesis, biological evaluation and molecular modeling study of substituted benzyl benzamides as CETP inhibitors. Arch Pharm 2017;350(12):1700204.
50. Khalaf RA, Awad M, Al-Qirim T, Sabbah D. Synthesis and molecular modeling of novel 3, 5-Bis (trifluoromethyl) benzylamino benzamides as potential CETP inhibitors. Med Chem 2022;18(4):417-26.
51. Khalaf RA, NasrAllah A, Jarrar W, Sabbah DA. Cholesteryl ester transfer protein inhibitory oxoacetamido-benzamide derivatives: Glide docking, pharmacophore mapping and synthesis. Braz J Pharm Sci 2022;58.
52. Schrödinger R. Protein preparation wizard, maestro, macromodel, QPLD-dock and Pymol. Schrödinger, LLC. 2016:97204.
53. Friesner RA, Banks JL, Murphy RB, Halgren TA, Klicic JJ, Mainz DT, *et al.* Glide: A new approach for rapid, accurate docking and scoring. 1. Method and assessment of docking accuracy. J Med Chem 2004;47(7):1739-49.
54. Friesner RA, Murphy RB, Repasky MP, Frye LL, Greenwood JR, Halgren TA, *et al.* Extra precision glide: Docking and scoring incorporating a model of hydrophobic enclosure for protein−ligand complexes. J Med Chem 2006;49(21):6177-96.
55. The Molecular Operating, Environment Chemical Computing Group. Inc.: Montreal, QC, Canada. 2016.